NASA-CR-191391

(NASA-CR-191391) FAILURE OF COMPOSITE PLATES UNDER STATIC BIAXIAL PLANAR LOADING Final Report (Michigan Univ.) 29 p

N93-15653

Unclas

G3/39 0135393

485037

College of Engineering

DEPARTMENT OF AEROSPACE ENGINEERING

The University of Michigan
Ann Arbor, Michigan 48109-2140

Failure of Composite Plates Under Static Biaxial Planar Loading

by

Anthony M. Waas (PI)
Amir R. Khamseh (Graduate Student)

NAG 1-1040

FINAL REPORT

December 18, 1992

NASA Langley Research Center
Contract No. NAG-1-1040
Program Monitor: Dr. M. J. Shuart

Composite Structures Laboratory
Department of Aerospace Engineering
College of Engineering
University of Michigan

Table of Contents

Abstract

This report describes the research work carried out during the period January, 1991 through December 1992, for the NASA Langley Research Center project NAG-1-1040, under the supervision of Dr. M. J. Shuart. It proceeds previous similar reports that disseminated results accomplished prior to January 1991.

The project involved detailed investigations into the failure mechanisms in composite plates as a function of hole size (holes centrally located in the plates) under static loading. There were two phases to the project, the first dealing with uniaxial loads along the fiber direction, and the second dealing with coplanar biaxial loading.

Results for the uniaxial tests have been reported and published [1] previously, thus this report will emphasize more on the second phase of the project, namely the biaxial tests. The composite plates used in the biaxial loading experiments, as well as the uniaxial, were composed of a single ply unidirectional graphite/epoxy prepreg sandwiched between two layers of transparent thermoplastic. This setup enabled us to examine the failure initiation and propagation modes non-destructively, during the test. Currently, similar tests and analysis of results are in progress for graphite/epoxy cruciform shaped flat laminates. The results obtained from these tests will be available at a later time.

List of Figures

1. Introduction

Recent advances in the manufacturing of fibrous composite materials, combined with their inherent high strength/stiffness to weight ratios, have given them a high priority in aerospace applications. However, due to the complex infrastructure of these materials, their behavior under loading has not been completely analyzed. Composite materials behave very differently under loading and in failure as compared to the traditional aerospace materials (i.e. metals such as steel and aluminum) which have a very predictable stress-strain behavior. Composite materials under loading exhibit a very quick and catastrophic progression of failure, rendering the material incapable of bearing any load. In the aerospace field composite plates are to be used, where these plates will come under loading (i.e. fuselage panels) and where the plates may have areas of high stress concentration (i.e. holes or cutouts) in them. This report outlines the experimental investigations carried out for the analysis of failure mechanisms in unidirectional composite plates with centrally located circular holes of varying size, under static uniaxial and biaxial loading.

Research into previous work carried out for biaxial loading of composite plates revealed very little published material on the subject [2-5]. The work that had been carried out indicated an empirical approach to the subject, rather than a mechanical approach. It was the purpose of this investigation to utilize a mechanical approach in determining the failure modes of composite plates under biaxial planar loading. In order to keep the analysis as broad and general as possible, simplified composite plates were used in the investigation. The difficulty arising from this analysis arises from the non-linearity in the biaxial loading of such plates. The loading path for composite plates under biaxial loading is path dependent, i.e. if an initial load P1 is applied along one axis of the plate, followed by a load P2 along the second axis, the behavior of the plate may be completely different than the case where the load P2 is applied along the second axis, followed by P1 along the first axis. For the investigation reported herein dealing with the single ply unidirectional composites, a single load ratio (2:1, where the loading in the fiber direction was twice that in the direction perpendicular to the fiber) was employed, with an in phase load path (i.e. both loads applied simultaneously from the start).

2. Experimental Details

An experimental analysis of the specially prepared uni-ply composite plates was carried out for uniaxial compressive loading, the results of which were reported in reference [1]. Experimental results revealed failure initiation to occur at the edge of the hole, in the form of fiber microbuckling/ kinking, followed by delamination, for specimens with hole sizes varying from the largest down to a cutoff hole size. Below this range, failure either initiated at the outer free edges, in the forms of cracks, or was in the form of global (total) delamination. An FEA incorporating classical lamination theory was carried out utilizing the measured material properties and geometries, in order to gain insight into the in-plane failure mechanisms evident in the experimental observations. The analysis modeled the graphite-epoxy uniply in an attempt to reproduce the results obtained experimentally. The FEA results agreed very well with the buckled mode shapes from the experimental results, although the estimated buckling loads were larger than those obtained from experiments, probably due to imperfections in loading and material composition in the experiments. The trends for buckling modes and loads agree quite well for the two phases, revealing the inverse behavior between buckling load and hole size.

Upon completion of the first experimental stage of the project, namely the analysis of the composite plates under uniform static compressive uniaxial loading, it was concluded that a specialized loading frame needed to be designed and constructed which would have the capability of applying a biaxial load, either for tension or compression, on the plate specimens. An extensive literature search revealed very limited data [2,3] involving biaxial loading in the form of tension/compression. Most of the investigations thus far involving biaxial loading usually involve a combination of tension and torsion [4], or tension and hydrostatic pressure on cylindrical specimens [5]. A review of available loading frames revealed too many limitations and it was concluded that a frame would be designed from scratch and ordered to be built. The resulting biaxial loading frame (see Fig. 1) was constructed from twin carbon-steel (16 pound weight carbon steel beams, with maximum carbon content of 0.25) I-beams which were welded and machined into an H-beam configuration. The operative dimensions of the frame are as follows: length of 72 inches, width of 36 inches, with a 20 inch square working "window".

The hydraulic actuators (total of 4) and electronics were purchased from Test Systems and Simulations, Inc. (TSS). The actuators are Vickers T-J Linear Electrohydraulic Servo Actuator (LESA) TS09 cylinders with a 5 inch bore and 6 inches of stroke pistons, capable of tensile/compressive loads of 50,000 pounds when mated to a 3000 psi. hydraulic pump. Each actuator is a single ended design with integral servovalve (SM4-20) manifold and Temposonic displacement transducer. It should be noted that each of the cylinders can be programmed with a load or displacement feedback controller (via the use of a load cell or LVDT), fully independent of the other three cylinders. Two load cells will be used in the system, one along each loading axis, each rated for 50,000 pounds in tension and compression. A study was carried out for the use of ball joints along the two axes of the load frame, similar to what was done in the uniaxial experiment, in order to ensure uniform loading, and the results were implemented in the present setup (see Fig. 2).

In order for the biaxial test system to make use of the hydraulic pump which was used in the uniaxial loading experiments, a manifold was designed and built to accommodate the branching out of the pressure and tank lines to the four actuators. A second pressure bladder accumulator was installed at the manifold, along with a dump valve in order to release the line pressure after shutdown. A port was drilled in case of a need for a second tank (or return) line bladder accumulator. Lines from the manifold to the actuators were hard piped (rated to 6000 psi. at the rate of flow of the pump used, 5GPM) to provide for a less cluttered working environment.

Final modifications to the test setup involved fine tuning of the electronic circuitry needed to drive the system, including ramp generators used in a load or displacement feedback test to control the movement of the pistons, as well as calibration of the existing electronic hardware made available with the actuators. Two load cells were used in the system, one along each loading axis, each rated for 50,000 pounds in tension and compression. For the case of the material of the Uni-ply composite plate investigated in the uniaxial experimental tests, the stress concentration factor at the hole edge due to the compressive stress edge loading was calculated to be 3.57. Using the same material, the stress concentration factor, at the top and bottom hole edges, for the plate specimen under biaxial compressive loading (ratio 2:1) would be 3.17.

For the case of the Uni-ply composite plate under biaxial compressive loading (with a loading ratio of 2 to 1, along and perpendicular to the fiber direction, respectively), a mesh model of the plate and grips was generated using the HKS/ABAQUS Finite Element Analysis (FEA) software package. The stress analysis program was used to examine the effect of several specimen and loading tab geometries on the stress concentrations due to the applied load. The loading ratio was introduced at the boundaries of the loading tabs through the use of displacement constraints. The FEA indicated the optimal shape to be a cruciform configuration, where optimal refers to a stress state for which the working area of the specimen does not see the effects of the edges of the plate due to the loading. In our work, the working area translates into a 2.500 inch square region in the middle of the cruciform configuration.

Several studies were carried out for the design geometry of the specimen grips, in order to assure for the constraints of the tests, namely alignment, rigidity, accessibility, ease of use, ease of mounting, and repeatability given the working area in the frame and the geometric limitations of the specimens (0.275 inch thick with 3.000x1.250 inch wide arms (see Figs. 3,4)). The final design that was implemented into the experimental work made use of four (one for each arm of the cruciform configuration of the specimens) aluminum grips (see Fig. 5) (same modulus of elasticity as that calculated for the Ultem composite plates) with a 3.000x1.500 inch polished base which would come in contact with the load cell mounting plates and ball joints. In the center of the grip, a 0.2850 inch channel 1.200 inches in depth was machined along the length of the grip. The specimen arm would sit in this channel, bonded to the walls of the channel with the use of Dev-Con adhesive, treated with release agent in order to allow for simple separation of the two material at the conclusion of the experiment. More importantly, the Dev-Con putty acted as an interface between the specimen edge and the grip surface on which the specimen 'sat', effectively smoothening out the interface surface irregularities between the two material and ensuring a smooth load transfer. To ensure proper alignment of the specimen inside the channel (i.e. ensuring perfectly centered seating seating of the specimen inside the channel), metal shim plates of various thicknesses were added to both sides of the specimen while inside the grip. As the grips were mated directly to the specimen and not to any portion of the test frame (see Fig. 6), the alignment of the test specimen inside the setup became crucial in avoiding bending effects under load. This was achieved by a two step process. First, the four pistons were aligned with respect to each other such that not only were they collinear, but also coplanar. Second, the bottom and left pistons were marked such that when the specimen/grips setup was placed inside the markings, alignment with respect to the loading axes would be assured.

3. Results and Discussion

A series of twelve biaxial compressive load tests were carried out for the unidirectional composites for a range of five hole sizes (2 specimens per hole size). The hole sizes were as follows: 0.160, 0.245, 0.333, 0.415, and 0.500 inches in diameter. All these hole sizes corresponded to a hole diameter to plate width aspect ratio which results in failure initiation at the edge of the hole in the case of the uniaxial tests. The 0.1600 inch hole diameter corresponded to the cutoff aspect ratio in the uniaxial case, the limit at which the failure mode changed from the hole edge to the far field global delamination. The experiments monitored loads (via the load cells) and strains (both at the hole edge and in the far field of the specimen (see Fig. 7)). Loading was displacement controlled, with all four pistons moving 0.15 inches, the pair along the 2 loading direction covering this distance in 1000 seconds and the other pair in twice the time.

In both cases for each of the 0.5000, 0.4150, 0.3330, 0.2450 inch hole sized specimens, failure initiated long the top and/or bottom edge of the hole (perpendicular to the fiber direction) traversing into the specimen in the form of fiber kinking/microbuckling followed by delamination (very much similar to the uniaxial failure mode). Once again, as in the case of the uniaxial experiments, several of these specimens exhibited failure in the form of fiber kinking/microbuckling with no evidence of delamination, or delamination growth lagging behind the kink tip, once again reinforcing our conclusion from the uniaxial results indicating fiber kinking preceding delamination. However, the notable difference between these results and the uniaxial tests was the *location* of failure initiation along the hole edge. Whereas in the uniaxial tests the failure initiation was centered along the top (and/or bottom) edge of the hole, in the biaxial tests the failure initiation was shifted away from the center of the hole (shifted either to the left or right) (see Fig. 8). The reason for this shift is thought to be caused by the loading ratio (in our case 2:1), i.e. is dependent on the load ratio along the two axes of the plate. Further investigation is needed in this area, since computation of the detailed stress field around the circumference of the hole is needed.

For the case of the smallest hole size (0.1600 inch hole diameter), one of the tests showed no sign of failure initiation at the hole edge, and the specimen failed due to global delamination initiated at the far field (along the arms parallel to the fiber direction). The other sample tested showed similar failure initiation, with delamination failure extending from the right hand side into the middle of the specimen, but was followed under further loading with failure initiation at the top edge of the hole (again shifted to one one side, see Fig. 9). This reinforces our original assumption about a cutoff limit in hole aspect ratio for the mode of failure initiation exhibited.

Figures 10 and 11 show the far field failure stress and strain for the ten specimens tested, respectively, as a function of the hole aspect ratio (hole diameter non dimensionalized with respect to the plate width, in our case the width of the plate arms = 3.000 inches). The far field failure stress is simply the load readings along the fiber (2 loading) directions normalized with respect to the cross sectional area carrying the load (widthxthickness of plate arms = 3.000x0.275 square inches). As can be seen from the graph, there is once again, as in the case of the uniaxial loading stresses, an inverse relationship between hole size and failure stress. The smaller the hole aspect ratio, the higher the stress the specimen can carry prior to failure. The difference in magnitude between the biaxial stresses and corresponding uniaxial tests with the same hole aspect ratio (biaxial stresses are much higher, by a factor of two) can be attributed to the loading in the direction perpendicular to the fiber, effectively reducing the stress concentration factor at the top and bottom edges of the hole as compared to a purely uniaxial loading. The hole failure strain values, obtained indirectly from strain gage readings at the hole from back to back gages (strains were obtained from the gages and then manipulated to obtain true strain readings at the hole edge, taking into account the finite width of the strain gage itself) show some scatter (strains from specimens with hole diameters of 0.332 and 0.416 inches each), but again a downward sloping trend can be seen with respect to hole aspect ratio and failure strain. Furthermore, failure strains from the biaxial tests agree quite well with those from the uniaxial tests [1] for respective hole sizes, indicating that failure strain is purely a function of hole size, irrespective of the loading ratio. Thus, it appears that strain at the hole edge and a measure of the gradient are sufficient to fully characterize failure initiation in laminates containing zero plies.

In all the tests, there was evidence of delamination at the grip edges (particularly along the fiber, or 2 loading, direction) well before hole failure initiated (as evidenced by the 'sound' emitted, following delamination), however, not only did the delamination not propagate past the gripped arms into the center of the specimen, it also did not affect the load carrying capability of the specimen, as evidenced by the load readings from the tests, which exhibited no drop in load until failure initiation at the hole edge. The only time the grip delamination extended into the specimen was the case for the smallest hole size, as explained above. Furthermore, we believe this problem to be partly due to a flaw in the grip design which did not make use of the full arm area of the specimens, and that has been corrected for the modified grips being machined for the NASA composites [see Fig. 12].

4. Future Work

With the results obtained so far, we are comfortable with the use of the loading frame in the experimental analysis of biaxial loading of composite plates. The system behaves as designed and is capable of providing the variations in loading feedback (load or displacement) as well as loading paths. Our next step is to investigate the effect of the load path on one of the hole sizes for the unidirectional composites under investigation. As reported in the results, there was a distinct pattern in the location of failure initiation for the 2:1 loading. We will examine whether this is a function of the load ratios or not.

The next step will involve the testing of the specially prepared composites provided to us by NASA (courtesy of Dr. M. J. Shuart, the program monitor), namely the 48 ply IM7/5260 graphite/epoxy composite plates, a total of 36 specimens categorized into three groups: quasi-isotropic $[+45/0/-45/90]_{6s}$, shear dominated $[\mp45/\pm45]_{6s}$, and $[(+45/0/-45/0)_2/+45/0/-45/90]_{2s}$. Each group has a pair of specimens for the five hole sizes used in the unidirectional composite biaxial tests, along with a pair with no hole sizes which will be used to characterize the material properties of the composites and compare with published data provided by NASA [6]. The compression grips used for the biaxial experiments will be modified both in design and material property (specifically, use of high strength Stress-Proof steel instead of aluminum) as shown in Fig. 12. The geometric modification should strengthen the rigidity of the grip in resisting any bending moments applied due to a possible misalignment in loading, thereby avoiding the unwanted possibility of opening the mouth of the grip channel.

5. References

1. Khamseh, A.R., and Waas, A.M., 1992, "Failure Mechanisms of Uniply Composite Plates with a Circular Hole Under Static Compressive Loading", *ASME Trans. J. Eng. Materials and Tech.*, Vol. 114, July 1992, pp. 304-310.

2. Daniel, I.M., 1980, "Behavior of Graphite/Epoxy Plates with Holes under Biaxial Loading", Experimental Mechanics, January, pp. 1-8.

3. Daniel, I.M., 1982, "Biaxial Testing of $[0_2/\pm 45]_s$ Graphite/Epoxy Plates with Holes", Experimental Mechanics, May, pp. 188 -195.

4. Francis, P.H., Walrath, D.E., Sims, D.F., and Weed, D.N., 1977, "Biaxial Fatigue Loading of Notched Composites", Journal of Composite Materials, Vol. 11, pp. 488-501.

5. Swanson, S.R., and Christoforou, A.P., 1986, "Response of Quasi-Isotropic Carbon/Epoxy Laminates to Biaxial Stress", Journal of Composite Materials, Vol. 20, pp. 457-471.

6. Gates, T.S., 1991, "Experimental Characterization of Nonlinear, Rate Dependent Behavior in Advanced Polymer Matrix Composites", Proceedings of the 1991 SEM Conference Spring, June 10-13.

NASA Support

The support, enthusiasm and encouragement received from the NASA Langley Research Center has served us in many ways. We are very grateful for this support and in particular wish to thank Dr. Mark J. Shuart, our program monitor, for his guidance, encouragement and patience throughout this project.

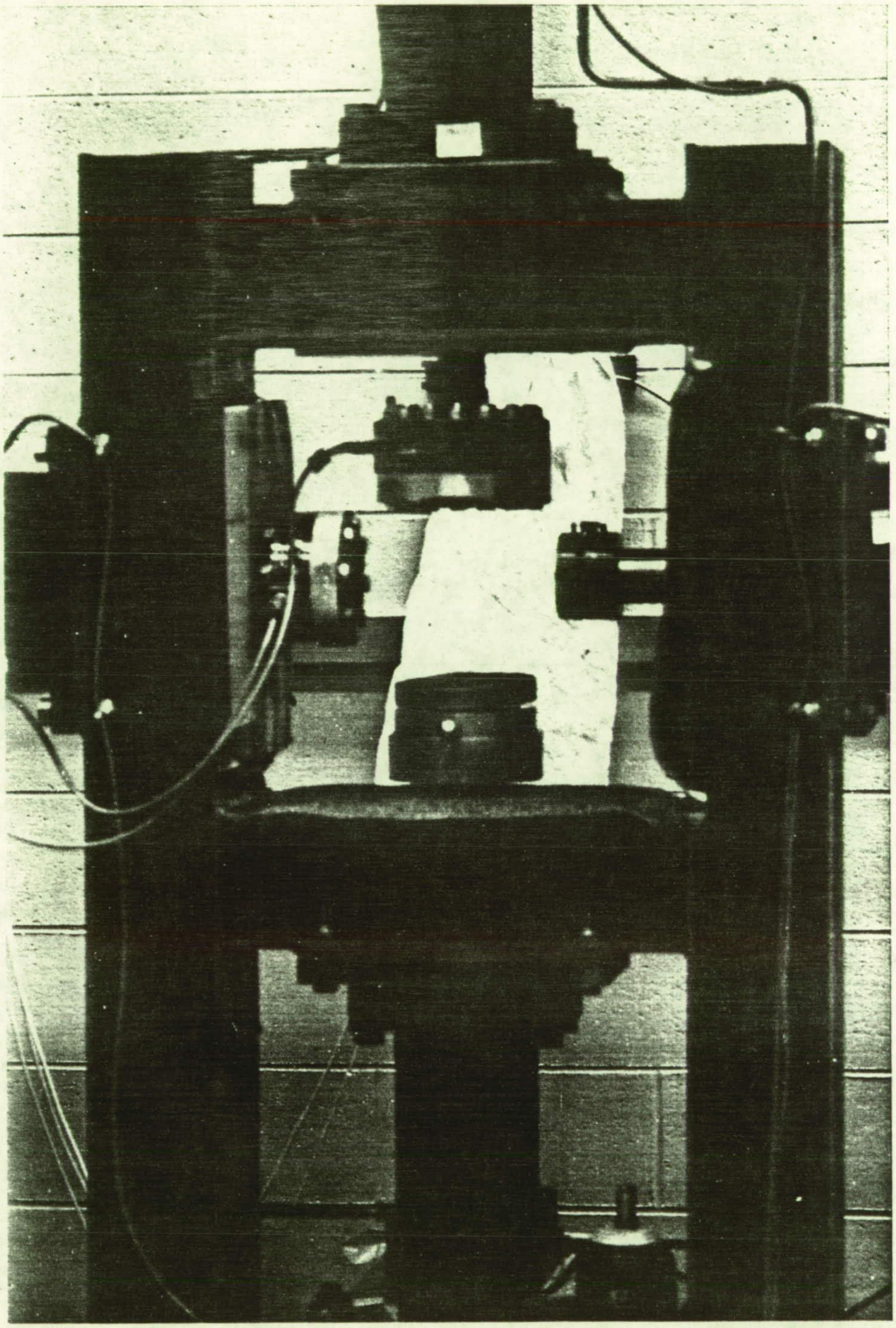

Fig. 1 Biaxial Loading Frame

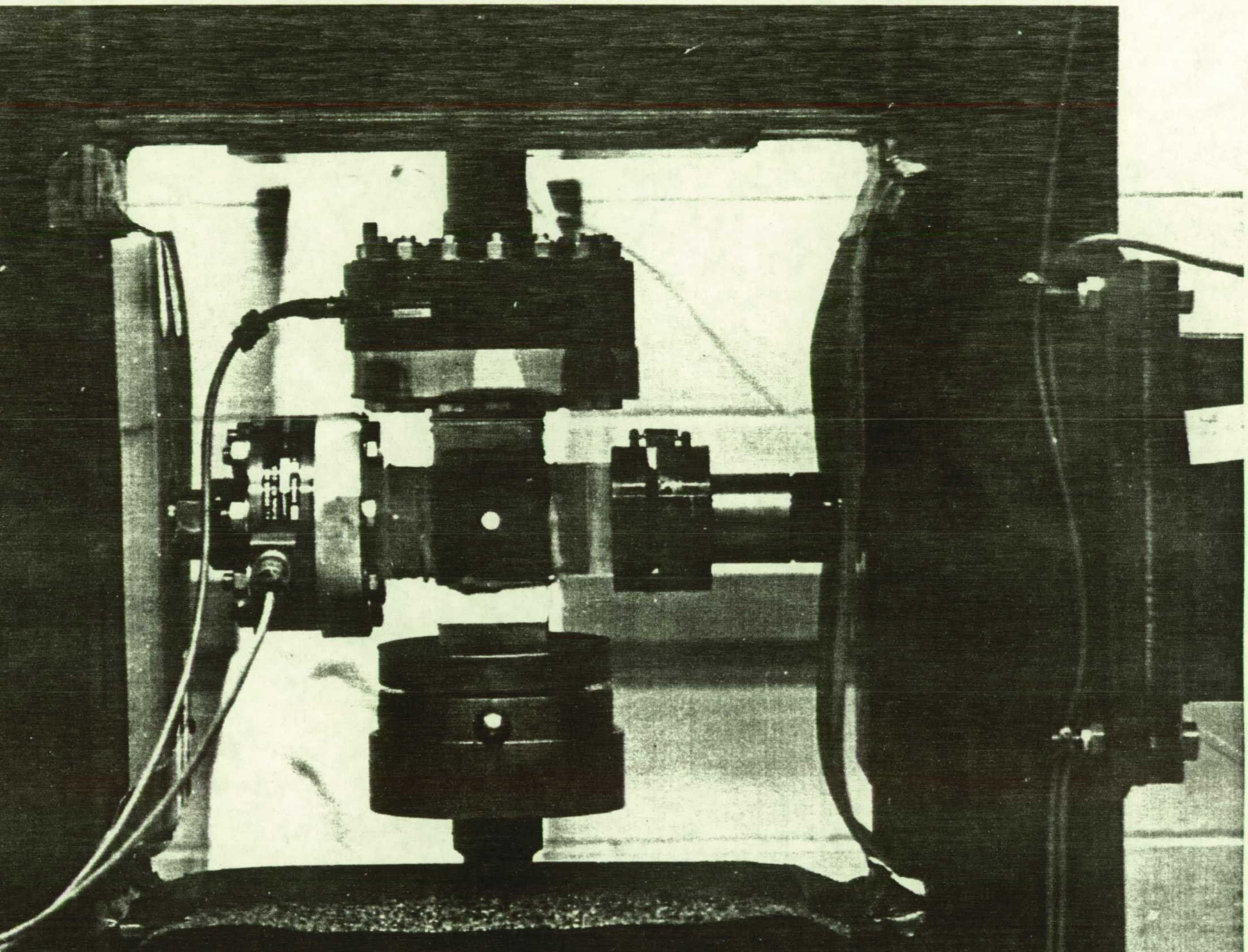

Fig. 2 Working Window in Frame

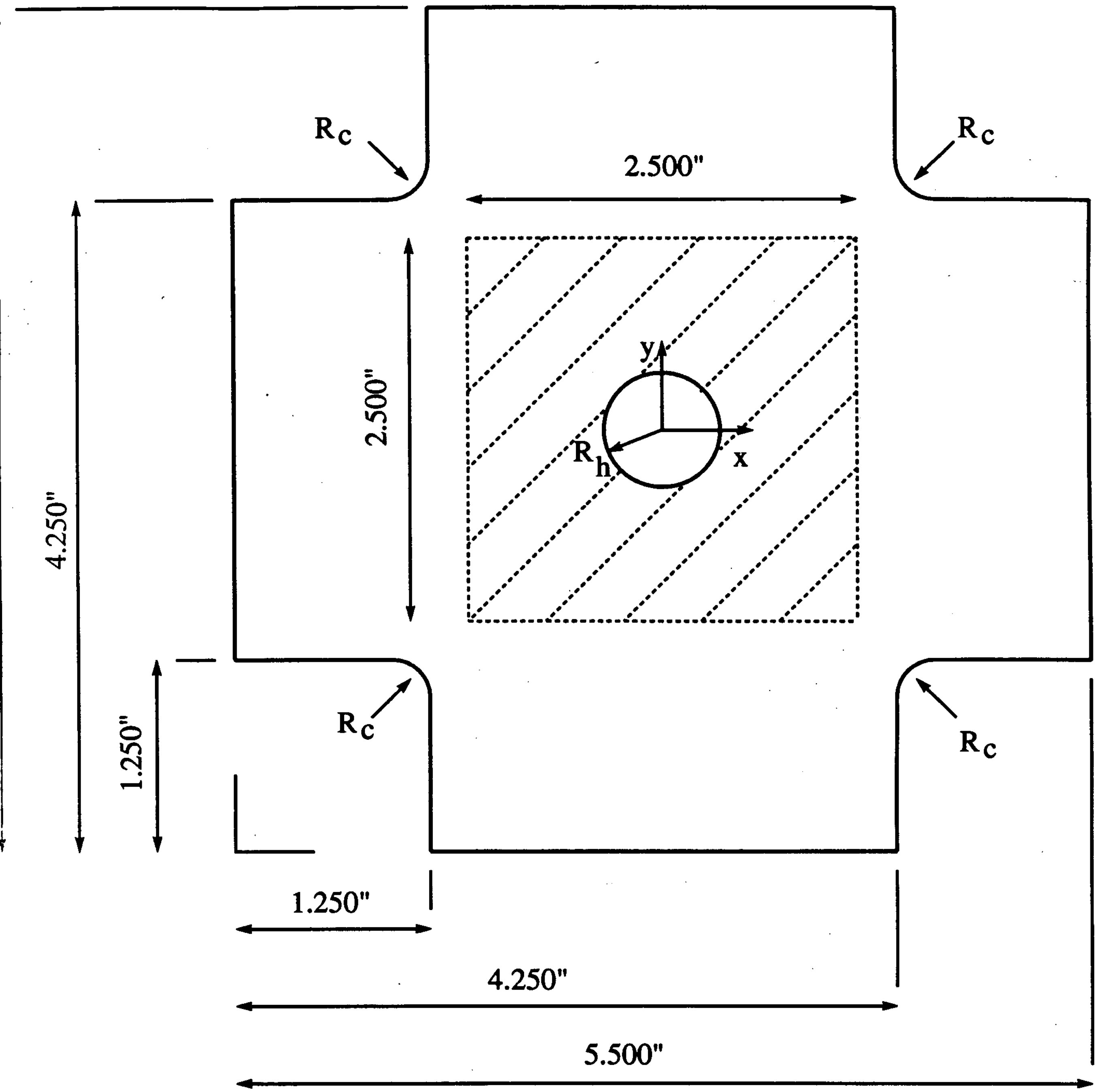

l dimensions are given in inches (+/- 0.005 inch tolerance)

)TE: Specimen is SYMMETRIC about the x and y axes

lius of curvature $R_c = 0.250"$

le radii $R_h =$ (0.0800", 0.1225", 0.1650", 0.2075", 0.2500")

Fig. 3 Specimen Configuration

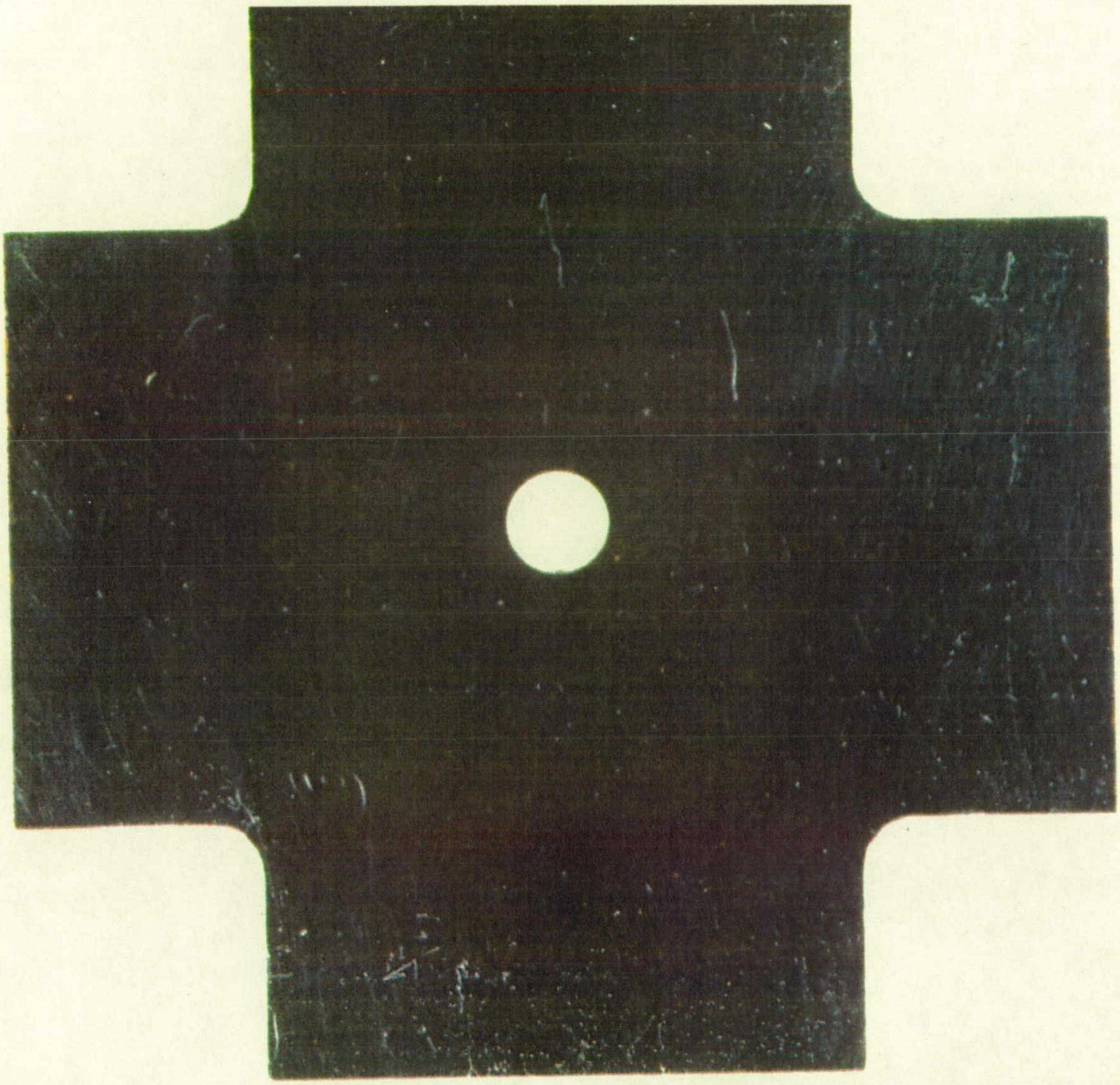

Fig. 4 Sample Composite Specimen

M
aterial: 6061-T6 Aluminum

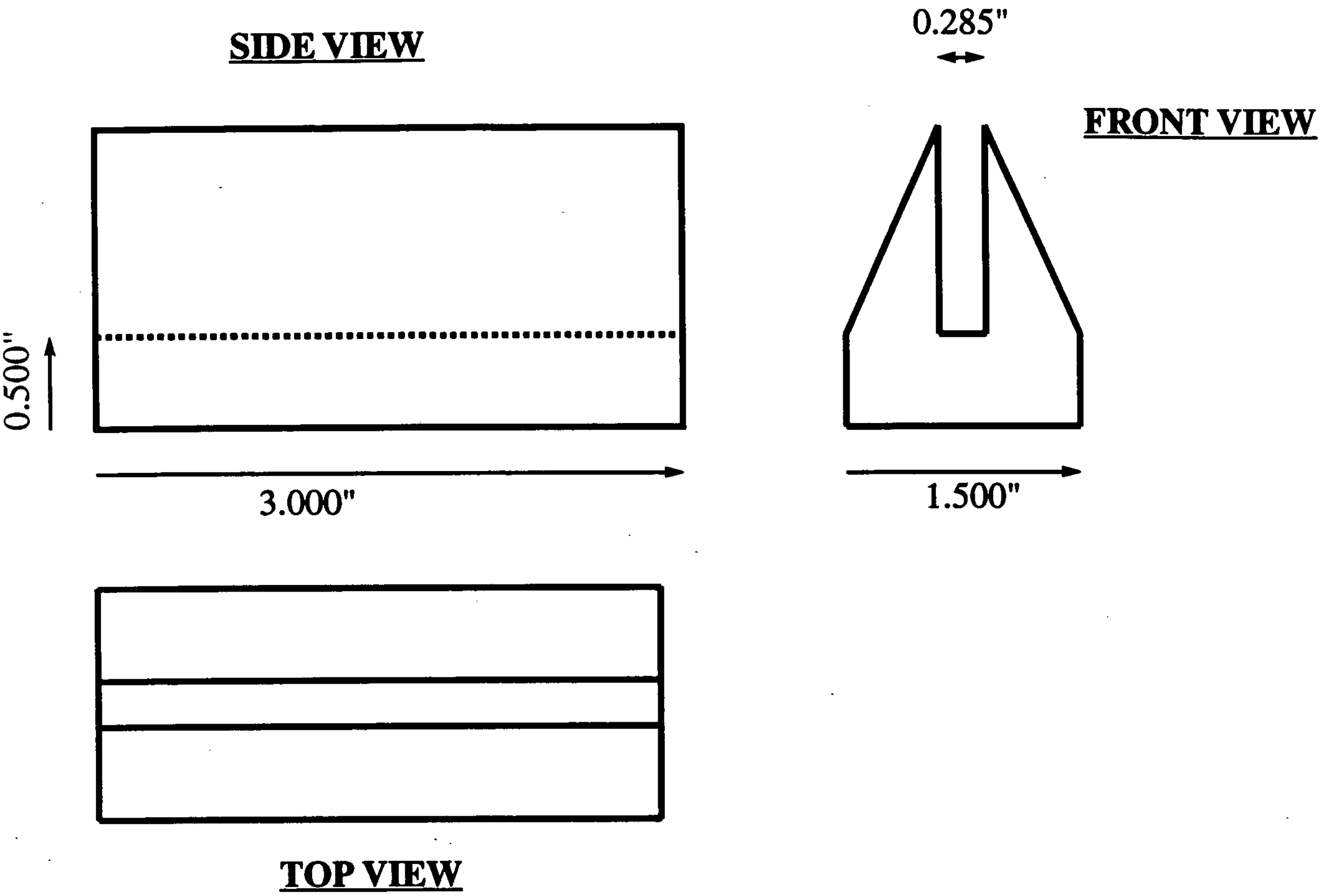

Fig. 5 Grips

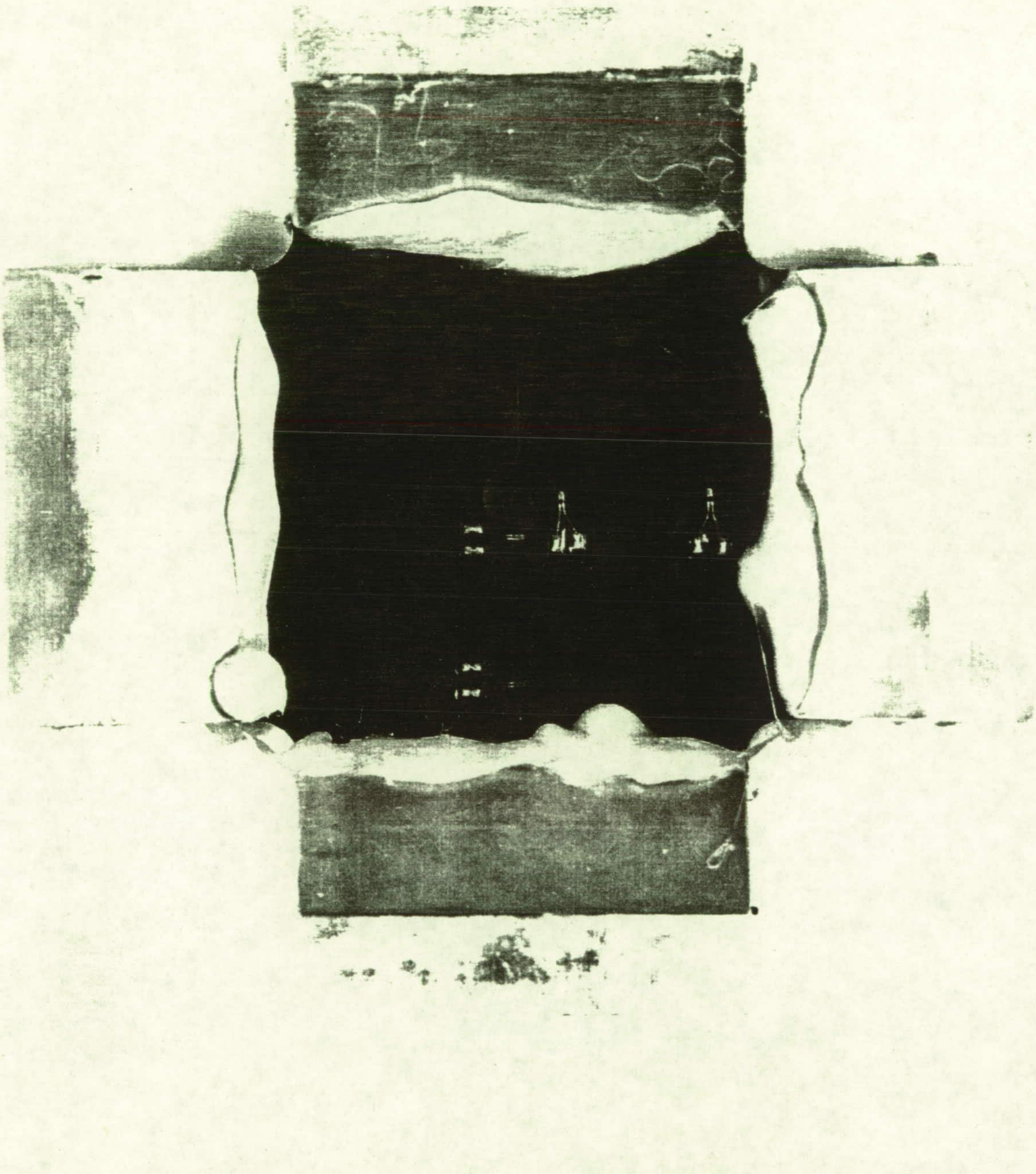

Fig. 6 Specimen in Grips

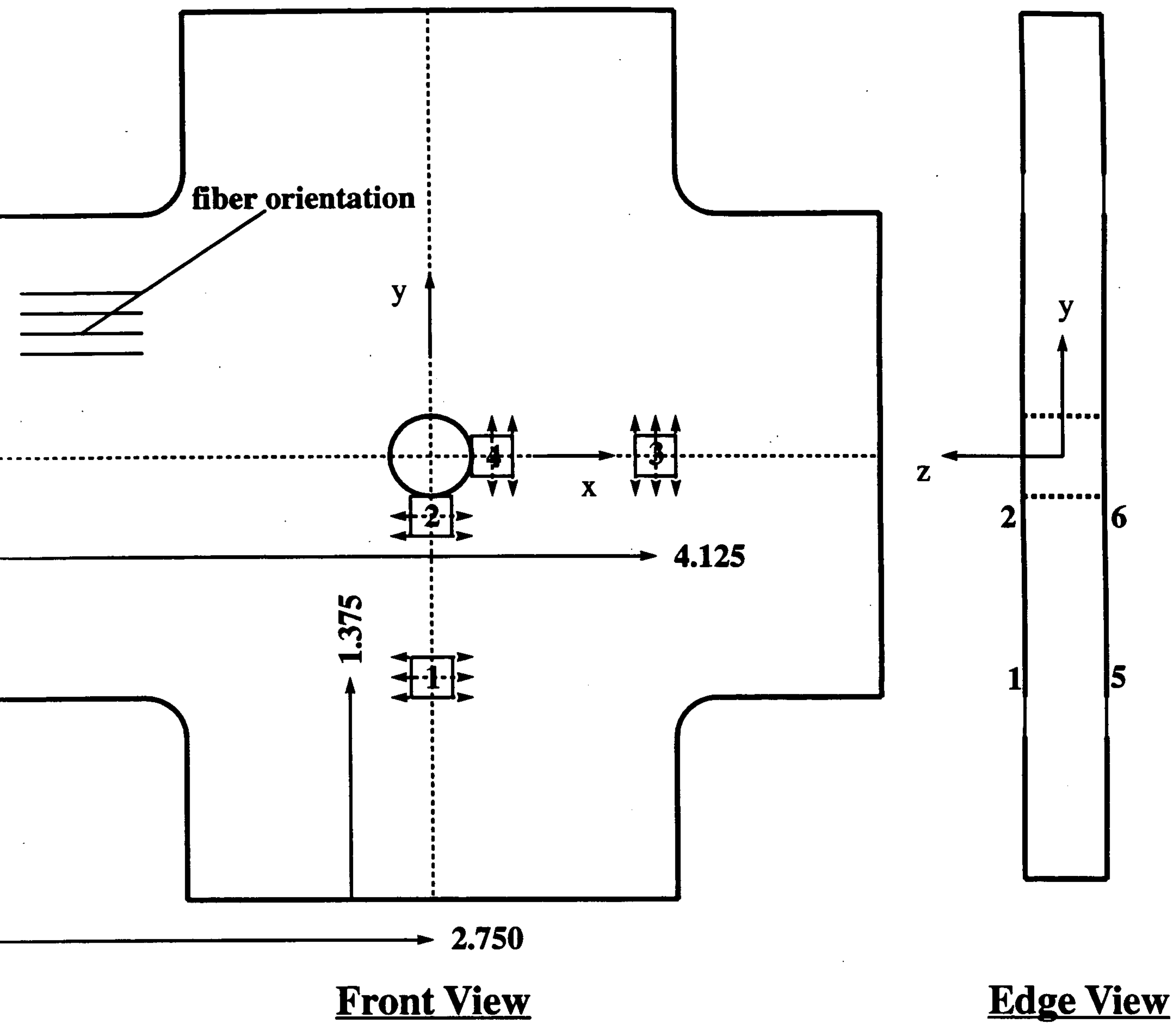

e: x,y-axes lie along the lines of symmetry (-----) of the specimen panel.

ain gages are paired (back to back) and placed along the lines of symmetry, hown in the above figure.

ection arrows (⟷) indicate the orientation of wiring in the strain gages.

dimensions shown in the above figure are given in units of inches.

nension lengths are measured to the midpoint of the respective strain gages.

Fig. 7 Strain Gage Positioning on Specimens

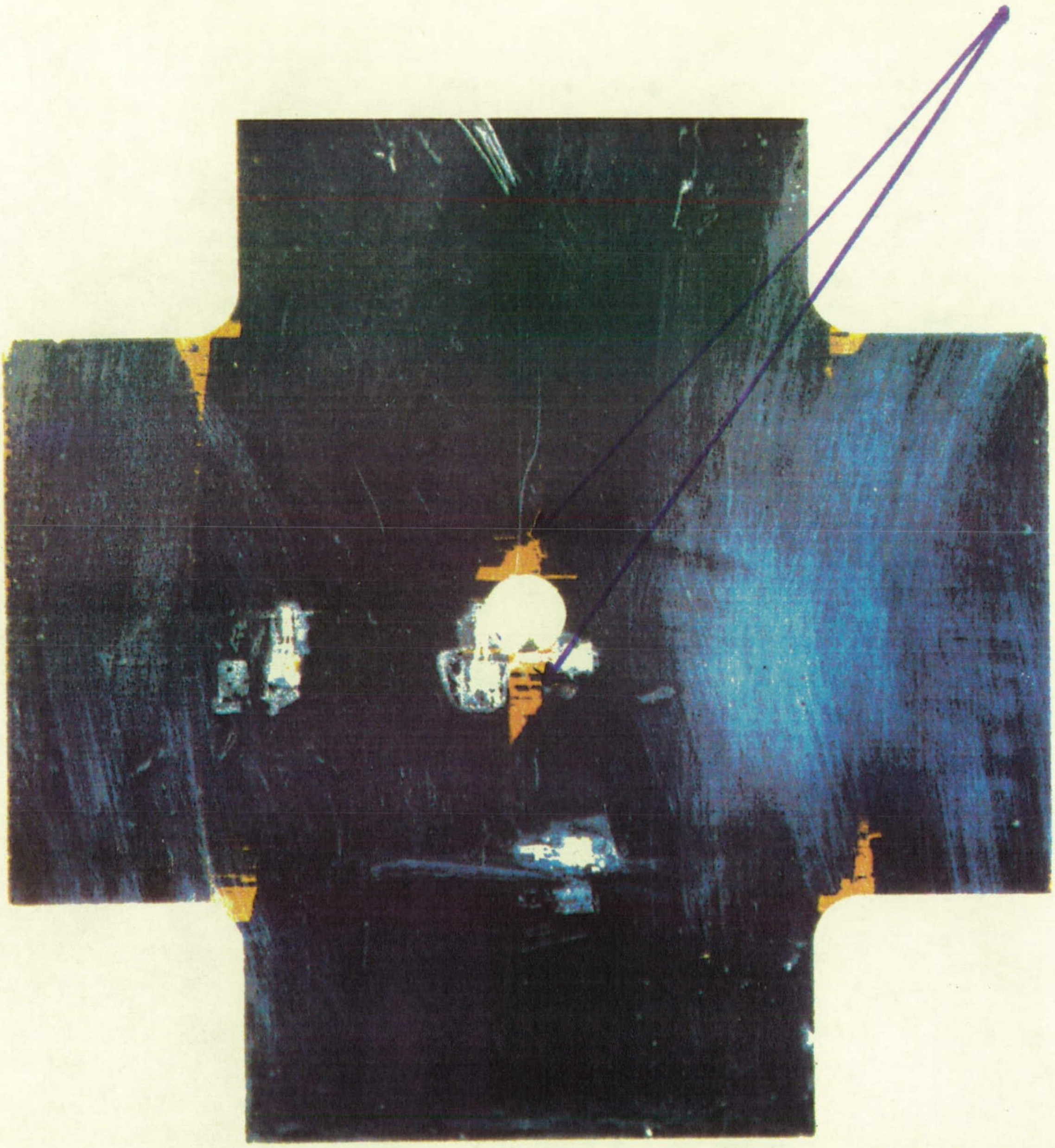

Fig. 8 Large Hole Size Failure Mode

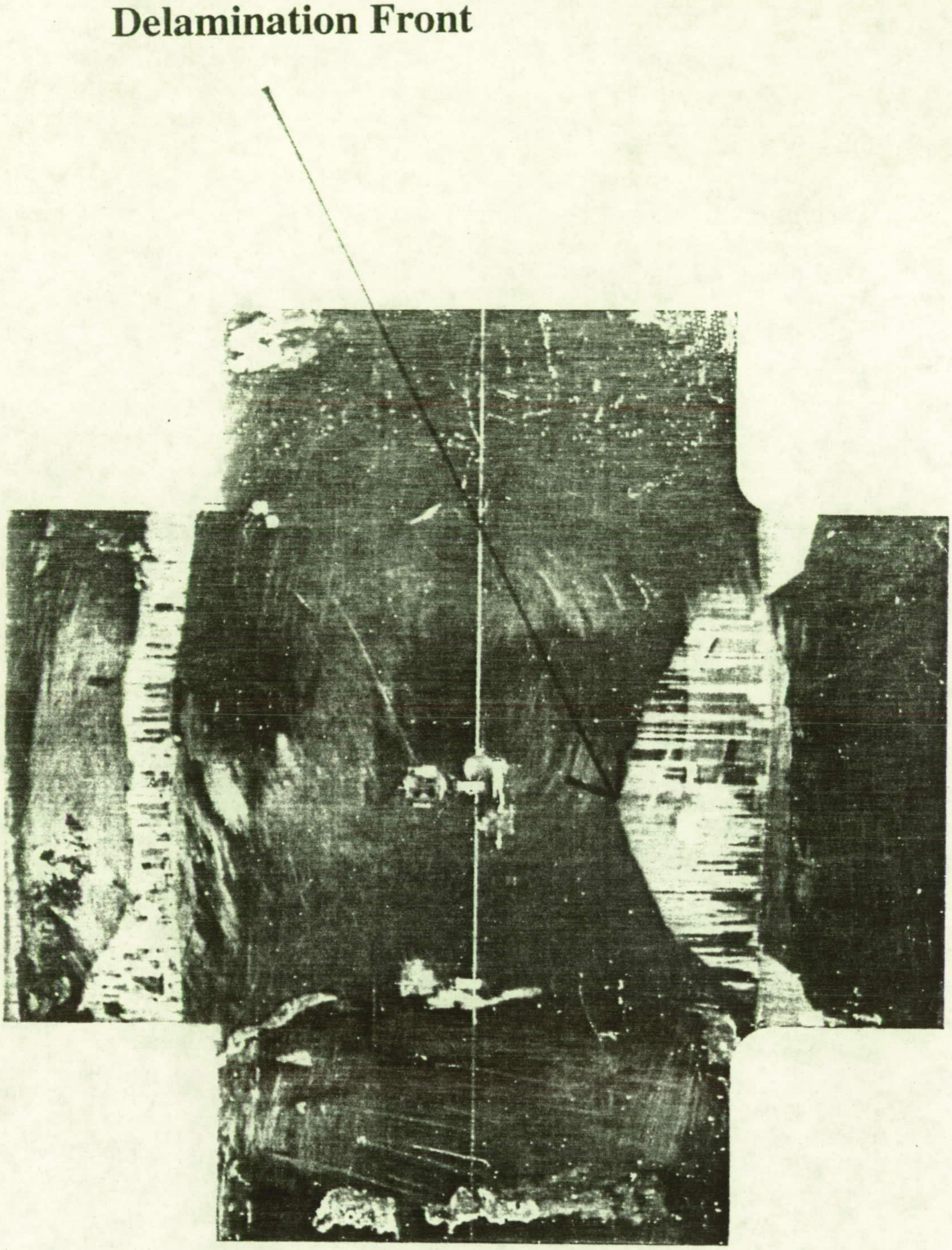

Fig. 9 Small Hole Size Failure Mode

Fig. 10 Far Field Failure Stress vs. Hole Size

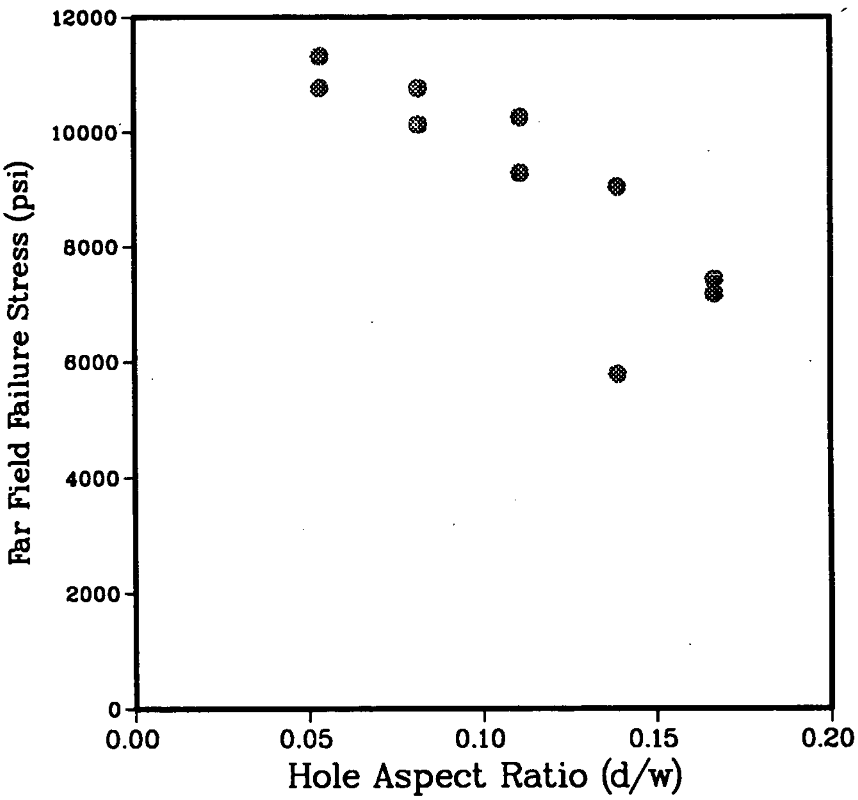

Fig. 11 Hole Failure Strain vs. Hole Size

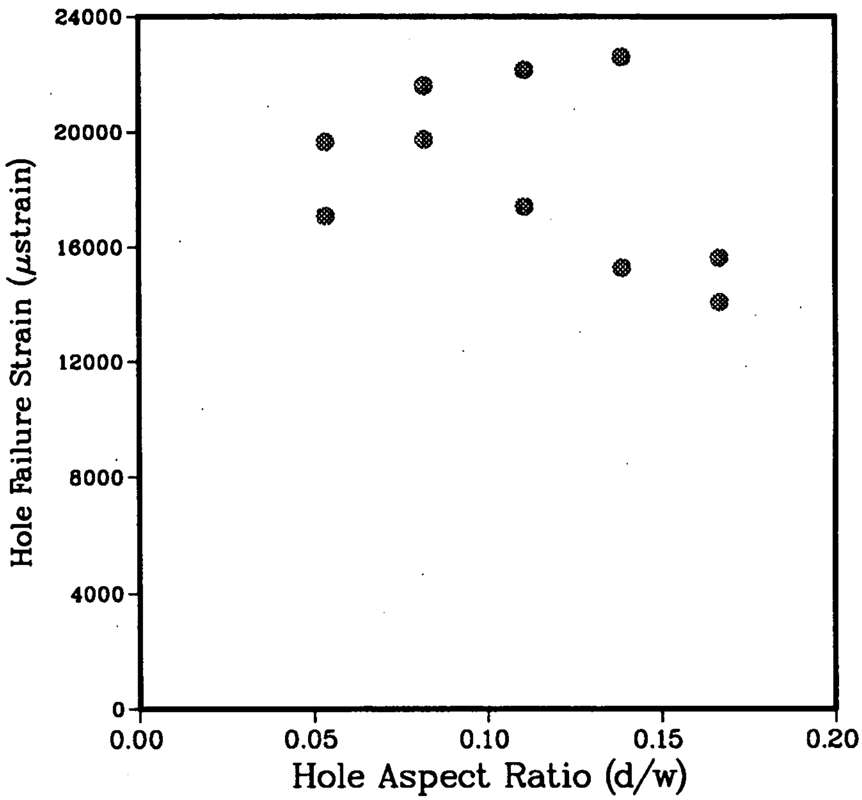

aterial: Stress Proof Steel
iantity: 4

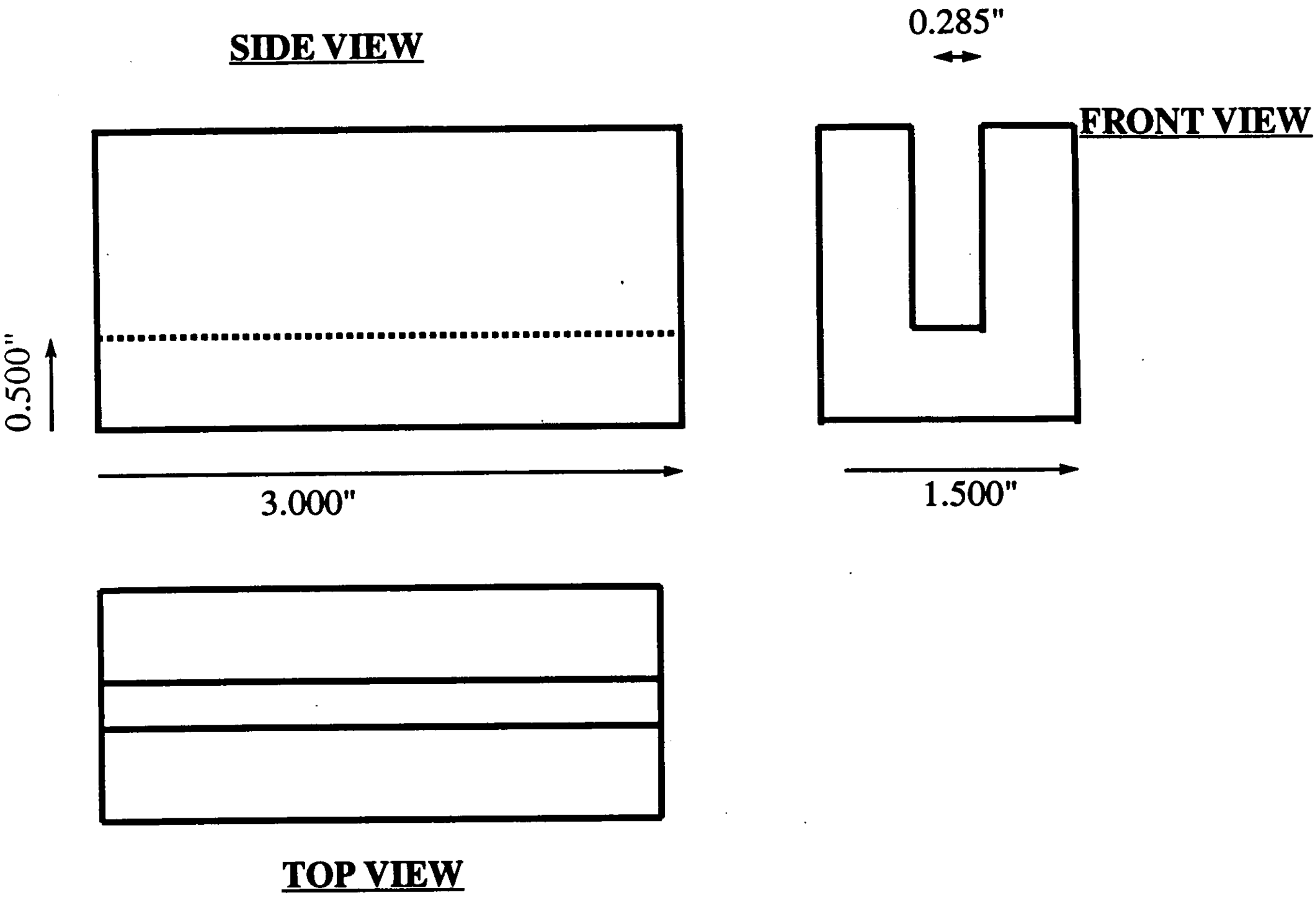

Fig. 12 Modified NASA Grips